JVI Journals.ASM.org

Vaccinia Virus Requires Glutamine but Not Glucose for Efficient Replication

Krystal A. Fontaine, Roman Camarda,* Michael Lagunoff

Department of Microbiology, University of Washington, Seattle, Washington, USA

ABSTRACT

Viruses require host cell metabolism to provide the necessary energy and biosynthetic precursors for successful viral replication. Vaccinia virus (VACV) is a member of the *Poxviridae* family, and its use as a vaccine enabled the eradication of variola virus, the etiologic agent of smallpox. A global metabolic screen of VACV-infected primary human foreskin fibroblasts suggested that glutamine metabolism is altered during infection. Glutamine and glucose represent the two main carbon sources for mammalian cells. Depriving VACV-infected cells of exogenous glutamine led to a substantial decrease in infectious virus production, whereas starving infected cells of exogenous glucose had no significant impact on replication. Viral yield in glutamine-deprived cells or in cells treated with an inhibitor of glutaminolysis, the pathway of glutamine catabolism, could be rescued by the addition of multiple tricarboxylic acid (TCA) cycle intermediates. Thus, VACV infection induces a metabolic alteration to fully rely on glutamine to anaplerotically maintain the TCA cycle. VACV protein synthesis, but not viral transcription, was decreased in glutamine-deprived cells, which corresponded with a dramatic reduction in all VACV morphogenetic intermediates. This study reveals the unique carbon utilization program implemented during poxvirus infection and provides a potential metabolic pathway to target viral replication.

IMPORTANCE

Viruses are dependent on the metabolic machinery of the host cell to supply the energy and molecular building blocks needed for critical processes including genome replication, viral protein synthesis, and membrane production. This study investigates how vaccinia virus (VACV) infection alters global cellular metabolism, providing the first metabolomic analysis for a member of the poxvirus family. Unlike most viruses examined to date, VACV does not activate glycolysis, and exogenous glucose is not required for maximal virus production. Instead, VACV requires exogenous glutamine for efficient replication, and inhibition of glutamine metabolism effectively blocks VACV protein synthesis. This study defines a major metabolic perturbation essential for the replication of a poxvirus and may lead to the discovery of novel antiviral therapies based on metabolic inhibitors.

All viruses rely on host cellular metabolism for the energy and macromolecule synthesis required for their replication. Recently, significant focus has been placed on examining how virus infection alters the host cellular metabolic profile in the hopes of identifying metabolic pathways that are critical to virus life cycles. Viral metabolomic analyses were first conducted to determine changes in host cell metabolism caused by human cytomegalovirus (HCMV) lytic infection (1, 2). HCMV was shown to induce multiple metabolic alterations, including upregulation of the tricarboxylic acid (TCA) cycle, fatty acid synthesis, pyrimidine nucleotide biosynthesis, and glycolysis. The metabolic effects of virus infection on human cells have now been investigated for several other viruses, including Kaposi's sarcoma-associated herpesvirus (KSHV), herpes simplex virus 1 (HSV-1), hepatitis C virus (HCV), human immunodeficiency virus (HIV), and dengue virus (1, 3–7). These studies have identified numerous metabolic perturbations induced by virus infection. Importantly, one metabolic alteration that has been observed in most of these reports is the activation of glycolysis, suggesting a role for glucose as a critical carbon source during virus infection.

Glucose and glutamine are the primary sources of carbon for energy homeostasis and biosynthesis in mammalian cells. Normally, glucose is considered the main contributor of cellular ATP through its oxidation via glycolysis and the TCA cycle. However, in cells where glucose carbon is being directed away from the TCA cycle, such as in most cancer cells and HCMV-infected cells, glutamine carbon can be used to replenish the TCA cycle, a process termed anaplerosis (2, 4, 8–11). Thus far, studies that have examined the impact of glucose and glutamine deprivation on virus production, including HCMV, HSV-1, and poliomyelitis virus, have found that both carbon sources are required for optimal viral replication (8, 12, 13).

Global metabolic analyses have not previously been performed on members of the *Poxviridae* family. Poxviruses are large, double-stranded DNA viruses that, in contrast to other DNA viruses, replicate entirely in the cytoplasm of infected cells (14). Vaccinia virus (VACV) is the prototypical poxvirus and was used as the live vaccine against variola virus, the causative agent of smallpox. Although smallpox has been eradicated, other poxviruses are able to

Received 29 October 2013 **Accepted** 24 January 2014

Published ahead of print 5 February 2014

Editor: K. Frueh

Address correspondence to Michael Lagunoff, Lagunoff@u.washington.edu.

* Present address: Roman Camarda, Department of Cell and Tissue Biology, University of California, San Francisco, California, USA.

Supplemental material for this article may be found at http://dx.doi.org/10.1128/JVI.03134-13.

doi:10.1128/JVI.03134-13

infect humans either exclusively or zoonotically to cause serious disease, including molluscum contagiosum virus and monkeypox virus (15–17). A highly pathogenic variant of monkeypox virus found in the Democratic Republic of Congo causes a smallpox-like disease and results in a mortality rate of approximately 10% (18, 19). Due to the potential use of variola virus as a bioterrorism agent, as well as the presence of other pathogenic poxviruses in the human population, furthering our understanding of poxvirus-host interactions remains an important challenge.

To identify perturbations in host cellular metabolic pathways during poxvirus infection, we performed a global metabolomic screen during a time course of VACV infection of primary human foreskin fibroblasts (HFFs). Of particular interest, data from this screen suggested that glutamine utilization is altered in VACV-infected cells compared to their mock-infected counterparts. Surprisingly, we found that exogenous glutamine is the critical carbon source for VACV replication and that glucose is dispensable for virus production. We also determined that glutamine, via its catabolism to α-ketoglutarate, is required to maintain the TCA cycle for VACV protein synthesis and that the loss of viral protein synthesis under glutamine-deprived conditions results in reduced levels of all virion morphogenetic intermediates. Therefore, VACV infection induces a dependence on glutamine metabolism to support efficient viral replication.

MATERIALS AND METHODS

Cells and viruses. Primary human foreskin fibroblasts (ATCC PCS-201-010) were propagated and maintained at 37°C in 5% CO_2 in Dulbecco's modified Eagle medium (DMEM) supplemented with 10% fetal bovine serum, 2 mM L-glutamine, 100 U/ml penicillin, and 100 μg/ml streptomycin. The VC-2 Copenhagen strain of vaccinia virus (obtained from Adam Geballe, Fred Hutchinson Cancer Research Center) was propagated in BSC40 cells (ATCC CRL-2761), and titers were determined by plaque assays on HFFs. For the glucose and glutamine depletion studies, DMEM lacking D-glucose, L-glutamine, sodium pyruvate, and phenol red (catalog number A14430-01; Invitrogen) was used. This medium was supplemented with 2% dialyzed fetal bovine serum (HyClone), and for replete medium, 1 g/liter D-glucose and 2 mM L-glutamine were added. Dialyzed serum was utilized in these studies, as it has been thoroughly depleted of small molecules, including glucose and glutamine. The glucose concentration reported for the lot of dialyzed HyClone serum used was <20 mg/dl; therefore, when used at 2%, there is <0.004 g/liter of glucose present in the medium.

Reagents and antibodies. Dimethyl-α-ketoglutarate (catalog number 349631), oxaloacetic acid (catalog number 04126), and pyruvate (catalog number S8636) were all purchased from Sigma and used at the indicated final concentrations. Bis-2-(5-phenylacetamido-1,3,4-thiadiazol-2-yl)ethyl sulfide (BPTES) (catalog number SML0601) was obtained from Sigma and solubilized in dimethyl sulfoxide (DMSO) to a stock concentration of 10 mM. Additional dilutions of BPTES were made in methanol and used at the indicated final concentrations. Anti-β-actin (catalog number A5441) was purchased from Sigma, and horseradish peroxidase-conjugated goat anti-mouse (catalog number 115-036-062) and goat anti-rabbit (catalog number 111-036-045) antibodies were purchased from Jackson ImmunoResearch.

Virus infections for metabolic analysis. HFFs grown to ~80 to 90% confluence were washed with Dulbecco's phosphate-buffered saline (DPBS) and serum starved overnight in DMEM. Cells were then mock or VACV infected (multiplicity of infection [MOI] of 3) in serum-free DMEM for 1 h, after which the inoculum was replaced with fresh serum-free DMEM. Cells were harvested at the indicated times with a cell scraper and washed once in cold DPBS, and pellets were snap-frozen in a dry ice-ethanol bath. Samples were stored at −80°C until shipment to Metabolon (Durham, NC).

A multitude of curation procedures were conducted by Metabolon to guarantee the quality of the data set presented. Metabolon data analysts used proprietary visualization and interpretation software to confirm peak identification consistency and to limit system artifacts, misassignments, and background noise among the various samples. Bradford assays (20) were performed to normalize all samples by protein concentration, and each biochemical in the mock samples was rescaled to yield a median of 1. Following log transformation and imputation with minimum observed values for each compound, two-way analysis of variance (ANOVA) with contrasts tests was used to determine which metabolites were significantly altered by VACV infection of HFFs at each time point across the 4 biological replicates. Error bars on metabolite-level line plot graphs reflect standard errors of the means from four separate infections.

Nutrient starvation and BPTES treatment studies. HFFs or BSC40 cells were washed with DPBS and infected with VACV at an MOI of 5 for 1 h. Cells were washed once with DPBS and fed replete medium, glutamine-free medium, or glucose-free medium. For experiments where TCA cycle intermediates were added to the medium, the final concentrations used were 7 mM dimethyl-α-ketoglutarate, 4 mM oxaloacetic acid, or 4 mM pyruvate. For BPTES treatment experiments, VACV-infected cells were fed replete medium containing methanol (control), 10 μM BPTES, or 10 μM BPTES and 7 mM dimethyl-α-ketoglutarate. Infected cells were harvested at 24 h postinfection (hpi) with a cell scraper, washed once in cold DPBS, and resuspended in 10 mM Tris-HCl (pH 9). Virus was released by subjecting the infected cells to three freeze-thaw cycles and sonication. Titers were determined by a plaque assay on BSC40 cells. Error bars reflect standard errors of the means from at least three separate experiments for the nutrient starvation and TCA intermediate rescue studies. Errors bars reflect standard errors of the means from two independent experiments for the BPTES treatment studies.

Cell viability assays. HFFs or BSC40 cells were washed once with DPBS and fed replete medium, glutamine-free medium, or glucose-free medium. Attached cells were removed by trypsinization at 24 h posttreatment and collected, along with the culture medium and DPBS wash containing any detached cells. Cells were concentrated, mixed 1:1 with 0.4% trypan blue solution, and counted with a hemacytometer. Error bars reflect standard errors of the means from three separate experiments.

Quantitative real-time reverse transcription-PCR (RT-PCR). Total RNA isolation and quantitative real-time PCR were performed as previously described (21), using 500 ng of total RNA from each sample for analysis. The primers used were E3L forward primer 5′-CGC AGA GAT TGT GTG TGA GG-3′, E3L reverse primer 5′-AAC GGT GAC AGG GTT AGC AC-3′, F17R forward primer 5′-ATT CTC ATT TTG CAT CTG CTC-3′, F17R reverse primer 5′-AGC TAC ATT ATC GCG ATT AGC-3′, hypoxanthine-guanine phosphoribosyltransferase (HPRT) forward primer 5′-GAA CGT CTT GCT CGA GAT GTG-3′, and HPRT reverse primer 5′-CCA GCA GGT CAG CAA AGA ATT-3′. Relative abundances of E3L mRNA and F17R mRNA were normalized by the delta threshold cycle method to the abundance of HPRT mRNA, with VACV-infected cells fed replete medium being set to 1. Error bars reflect standard errors of the means from three separate experiments.

Western blot analysis. Mock- and VACV-infected cells were harvested by trypsinization and lysed in radioimmunoprecipitation assay (RIPA) buffer (50 mM Tris-HCl [pH 7.6], 150 mM NaCl, 1 mM EDTA, 1% NP-40, 0.5% deoxycholate, 0.1% sodium dodecyl sulfate) supplemented with protease and phosphatase inhibitors. Proteins were separated by SDS-PAGE (7.5% polyacrylamide gels) and transferred onto Immobilon P polyvinylidene difluoride membranes (Millipore). Blots were incubated with the indicated primary antibody (dilutions of 1:4,000 for anti-E3L, 1:8,000 for anti-P4a, and 1:10,000 for anti-β-actin) and subsequently incubated with horseradish peroxidase-conjugated secondary antibody (dilutions of 1:20,000 for goat anti-rabbit and 1:30,000 for goat anti-mouse). Immunoreactive proteins were visualized by chemiluminescence using Amersham ECL Plus Western blotting detection reagents (GE

Healthcare Life Sciences). Differences in band intensity were quantified by densitometric methods using ImageJ (22).

Transmission electron microscopy. HFFs grown to ~80 to 90% confluence in 150-cm^2 cell culture flasks were infected with VACV at an MOI of 5 and fed replete medium, glutamine-free medium, or glutamine-free medium supplemented with 7 mM dimethyl-α-ketoglutarate. Infected cells were fixed at 24 hpi and processed for transmission electron microscopy (TEM). Briefly, VACV-infected cells were fixed with 2% paraformaldehyde and 2.5% glutaraldehyde in 0.2 M cacodylate buffer and were postfixed in 2% aqueous osmium tetroxide–0.2 M cacodylate buffer for 2 h at 4°C. After multiple washes, the samples were dehydrated in ethanol and embedded in Epon. Ultrathin sections were placed onto grids and stained with uranyl acetate and lead citrate. Samples were observed under a JEOL JEM-1400 transmission electron microscope (Fred Hutchinson Cancer Research Center electron microscopy facility) with a Gatan Ultrascan 1000XP camera and DigitalMicrograph software (Gatan, Pleasanton, CA).

Statistical analysis. Standard errors of the means are shown, and statistical differences between groups were analyzed with Student's *t* test or one-way ANOVA. A *P* value of ≤0.05 was considered significant and is indicated by an asterisk in the figures. A *P* value of ≤0.01 is indicated by a double asterisk, and a *P* value of <0.0001 is indicated by a triple asterisk in the figures.

RESULTS

VACV infection alters glutamine metabolism. To examine changes in host cell metabolism induced during VACV infection, we utilized a global intracellular metabolic profiling approach. Primary human foreskin fibroblasts (HFFs) were used for these experiments, as they are a commonly employed VACV-permissive primary cell type. Transformed cells are known to exhibit fundamentally altered metabolism; therefore, many transformed cell lines are often of limited value for examining virus-induced metabolic alterations (reviewed in references 10, 23, and 24). HFFs were serum starved for approximately 18 h prior to infection to synchronize the cells in the G_0/G_1 phase. Cells were then mock or VACV infected at an MOI of 3 and harvested at 4, 8, 12, and 24 h postinfection (hpi) for metabolic analysis. Samples from four independent experiments were analyzed by using both gas chromatography-mass spectrometry (GC-MS) and liquid chromatography-tandem mass spectrometry (LC-MS/MS). Our metabolomic screen identified numerous changes in host cellular metabolic pathways following VACV infection of HFFs (see Data Set S1 in the supplemental material). Interestingly, we noted a striking perturbation in glutamine metabolism during the course of VACV infection. Glutamine is metabolized via glutaminolysis, a process consisting of two deamination steps. In the first step, glutamine is deaminated to glutamate. The second deamination reaction then converts glutamate to α-ketoglutarate, an intermediate that can enter the TCA cycle. Figure 1A shows that both glutamine and glutamate levels were elevated in VACV-infected cells at multiple time points postinfection. Glutamine levels were significantly elevated in VACV-infected cells at both 4 and 8 hpi, whereas glutamate was found at increased levels in VACV-infected cells at all four time points examined. The metabolite α-ketoglutarate was not one of the 282 biochemicals detected in our samples. These data suggest that VACV infection alters glutamine utilization in HFFs.

Glutamine is required for maximal infectious VACV production. Because our metabolic screen identified an alteration in glutamine metabolism during VACV infection, we hypothesized that glutamine may be essential for viral replication. To test this, we investigated the impact of both glutamine and glucose deprivation on VACV production. HFFs were infected with VACV at an MOI of 5 and subsequently fed replete medium containing both glucose and glutamine or medium lacking either glucose or glutamine. At 24 hpi, cell-associated viral yields were determined by a plaque assay. As shown in Fig. 1B, depriving VACV-infected cells of exogenous glutamine reduced the production of infectious virus by approximately 90%. Surprisingly, starving VACV-infected cells of glucose had no significant impact on viral replication. Importantly, in the time frame examined for infection, the small changes observed in the growth and viability of uninfected HFFs under conditions of glutamine or glucose deprivation were similar, indicating that the block in VACV production was not due to the effects of glutamine deprivation on cellular integrity (Fig. 1C). While it was previously reported that HFFs lose viability when starved of glucose for 48 h (8), this was not the case following 24 h of glucose deprivation. These results reveal a dependence on glutamine, but not on glucose, during VACV infection.

In addition, we examined the impact of glutamine deprivation on VACV production in the permissive BSC40 cell line. As shown in Fig. 1D, starving VACV-infected BSC40 cells of exogenous glutamine resulted in an approximately 2-log reduction in viral yield. The observed block in VACV replication was not due to decreased cell viability under conditions of glutamine deprivation (Fig. 1E). Titers could not be accurately measured for glucose-deprived infected BSC40 cells, as they are a transformed cell line and are highly sensitive to glucose starvation, exhibiting ~17% cell death following glucose starvation for 24 h (reviewed in references 10, 25, and 26). However, even with this significant impact on cellular integrity, it is interesting to note that viral yields obtained from glucose-starved infected BSC40 cells were still more than a log higher than those obtained from glutamine-starved infected BSC40 cells (data not shown). This set of experiments further implicates that glutamine is the critical carbon source for VACV replication and that the requirement for glutamine is not cell type specific.

Glutamine is an anaplerotic substrate for the TCA cycle during VACV infection. Many cancer cell types utilize exogenous glutamine, via its conversion to α-ketoglutarate, to fill the TCA cycle. This anaplerotic usage of glutamine allows the cell to use glucose-derived carbon for biosynthetic purposes instead of energy production (9–11) (Fig. 2A). Similarly, it has been shown that HCMV-infected HFFs become dependent on glutamine to replenish the TCA cycle so that glucose carbon can be used primarily for fatty acid synthesis (8, 27). Our data indicate that glucose is not necessary for VACV replication, thus suggesting that a different carbon source is used to feed the TCA cycle during VACV infection. To determine if VACV-infected cells require glutamine to maintain the TCA cycle, we added a number of TCA cycle intermediates to the medium of glutamine-deprived infected cells. Following infection, HFFs were fed replete medium, glutamine-free medium, or glutamine-free medium supplemented with 7 mM dimethyl-α-ketoglutarate, 4 mM oxaloacetic acid, or 4 mM pyruvate. Cells were harvested at 24 hpi, and viral yields were measured by a plaque assay. The addition of exogenous TCA cycle intermediates to glutamine-deprived infected cells significantly rescued VACV production (Fig. 2B).

We also examined infectious virus production following pharmacological inhibition of glutaminolysis. VACV-infected cells were treated with bis-2-(5-phenylacetamido-1,3,4-thiadiazol-2-yl)ethyl

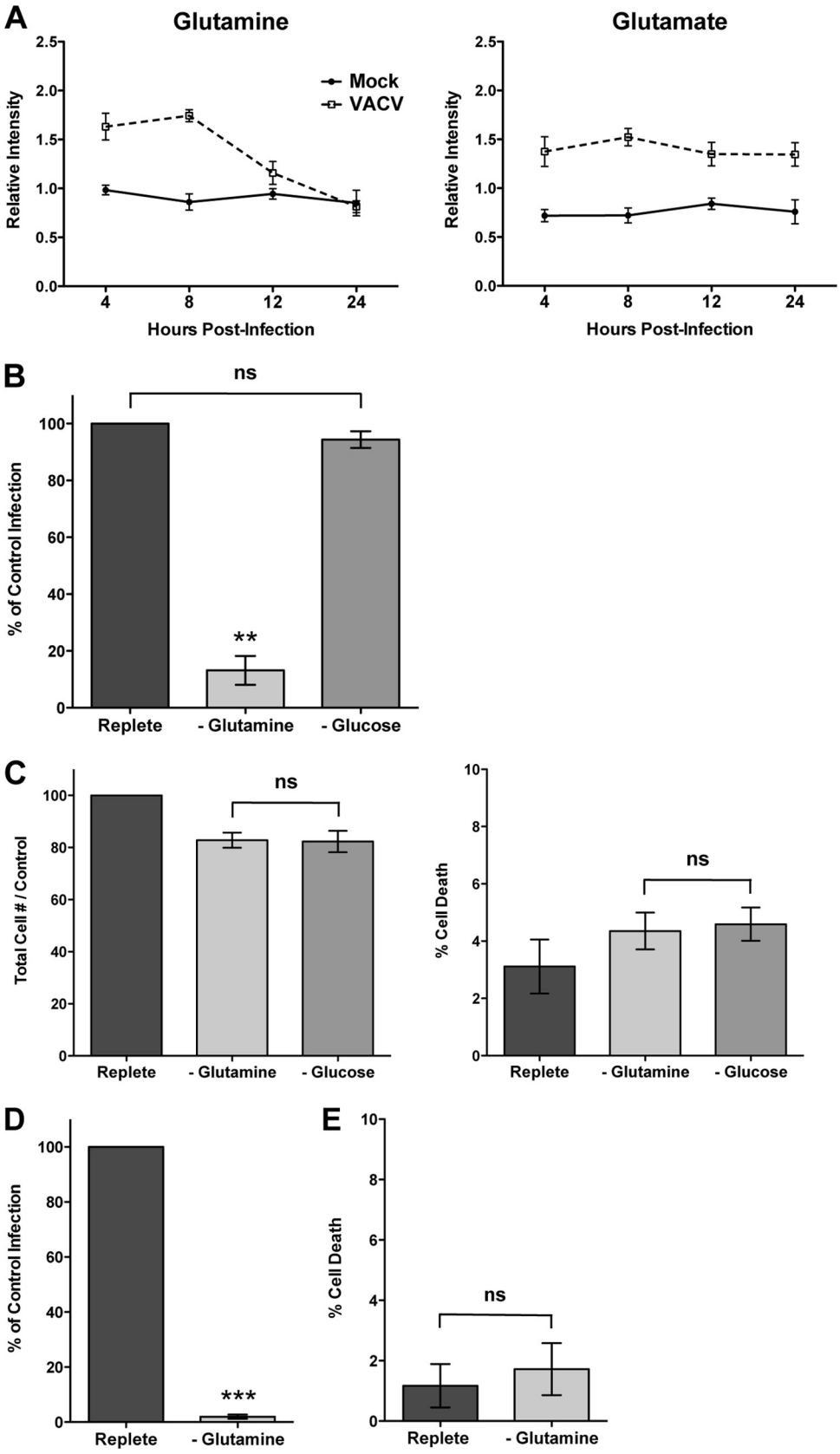

FIG 1 Glutamine is necessary for optimal infectious VACV production. (A) Line plots of glutamine and glutamate levels in mock- and VACV-infected cells measured at 4, 8, 12, and 24 hpi. Cells were harvested at the indicated time points, and Metabolon performed global metabolic analysis of the samples. (B and D) HFFs (B) or BSC40 cells (D) were infected with VACV at an MOI of 5 and were fed replete medium, glutamine-free medium, or glucose-free medium at 1 hpi. Cell-associated virus was harvested at 24 hpi, and viral yields were determined by a plaque assay. (C and E) HFFs (C) or BSC40 cells (E) were fed replete medium, glutamine-free medium, or glucose-free medium. At 24 h posttreatment, cell counts were determined, and viability was measured by using trypan blue exclusion staining. ns, not significant.

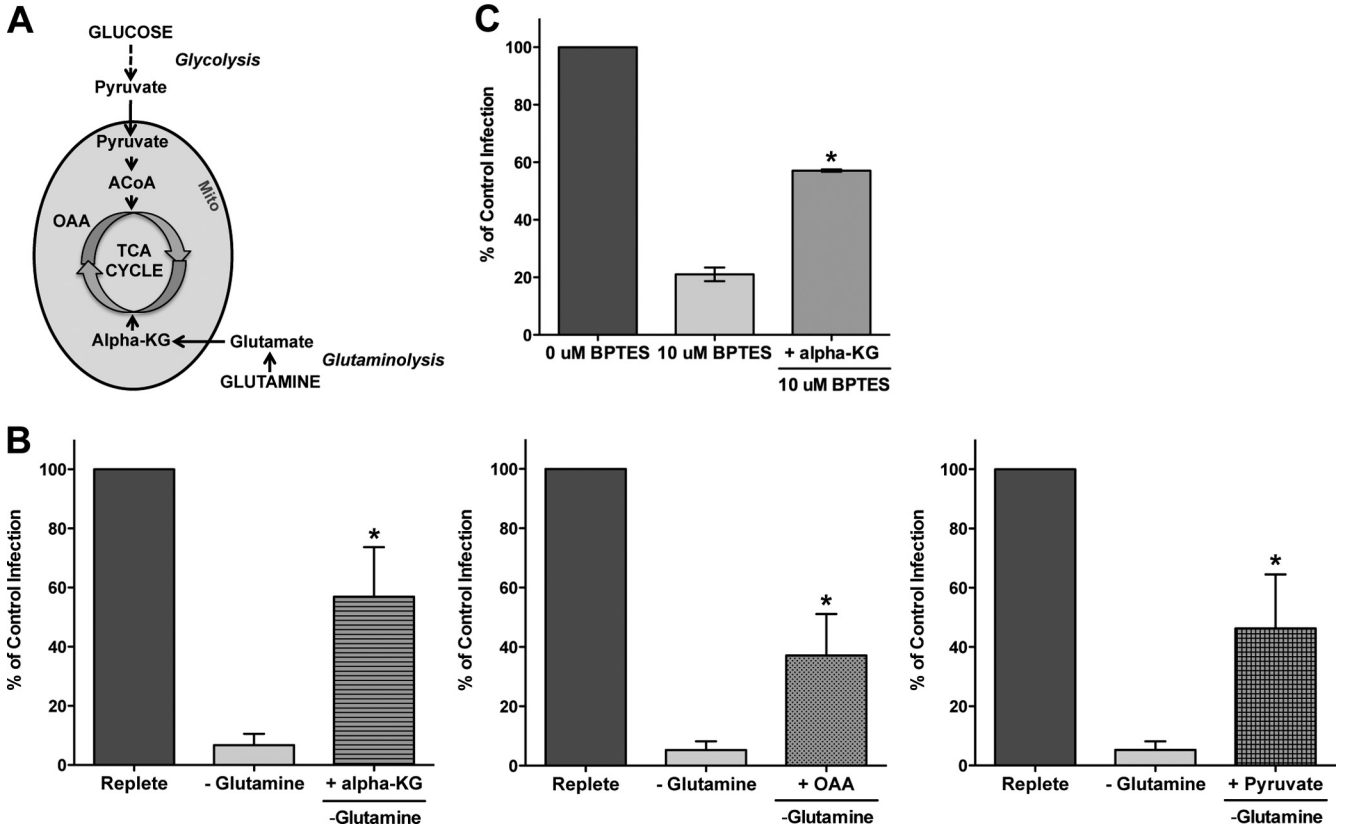

FIG 2 Glutamine is an essential anaplerotic substrate for the TCA cycle during VACV infection. (A) Simplified schematic of glucose and glutamine utilization. The dashed arrow represents multiple enzymatic reactions within the metabolic pathway. Abbreviations: alpha-KG, α-ketoglutarate; OAA, oxaloacetic acid; ACoA, acetyl coenzyme A. (B and C) HFFs were infected with VACV at an MOI of 5 and were fed replete medium, glutamine-free medium, or glutamine-free medium supplemented with 7 mM dimethyl-α-ketoglutarate, 4 mM oxaloacetic acid, or 4 mM pyruvate (B) or fed replete medium with 0 μM BPTES, 10 μM BPTES, or 10 μM BPTES and 7 mM dimethyl-α-ketoglutarate (C) at 1 hpi. Cell-associated virus was collected at 24 hpi, and viral yields were determined by a plaque assay.

sulfide (BPTES), a small-molecule inhibitor of glutaminase, the enzyme that catalyzes the first step of glutaminolysis, the conversion of glutamine to glutamate. Figure 2C shows that blocking of glutaminolysis reduced viral yields to levels similar to those obtained from glutamine-deprived infected cells. Moreover, virus production in BPTES-treated cells was significantly recovered by α-ketoglutarate supplementation. Combined, these data indicate that exogenous glutamine, via its conversion to α-ketoglutarate, is required to replenish the TCA cycle in VACV-infected cells.

Glutamine is necessary to maintain the TCA cycle for viral protein synthesis. To identify at what stage in the VACV life cycle glutamine is required, we first examined viral mRNA synthesis by quantitative real-time RT-PCR. For this experiment, we measured transcript levels of the VACV early gene E3L, which encodes an antagonist of the innate immune response, and the VACV late gene F17R, which encodes a protein involved in mature virion (MV) assembly. HFFs were infected with VACV at an MOI of 5 and fed replete medium or glutamine-free medium. Total RNA was isolated from infected cells harvested at both 2 hpi and 8 hpi, and quantitative real-time RT-PCR was conducted by utilizing primers specific for E3L and F17R. Figure 3A shows that E3L and F17R mRNA synthesis was not inhibited at either time point postinfection under glutamine-deprived conditions. These results indicate that exogenous glutamine is not required for VACV transcription.

We next examined early and late VACV protein expression via Western blot analysis. For this experiment, we measured the protein levels of the early gene E3L as well as the late gene P4a, which encodes the major VACV core protein precursor. Following infection, HFFs were fed replete medium, glutamine-free medium, or glutamine-free medium supplemented with either 7 mM dimethyl-α-ketoglutarate or 4 mM pyruvate, two TCA cycle intermediates that rescued infectious VACV production in glutamine-deprived cells (Fig. 2). As shown in Fig. 3B, early and late viral protein synthesis was blocked when VACV-infected cells were starved of exogenous glutamine. E3L and P4a protein levels were substantially recovered by the TCA cycle intermediate α-ketoglutarate or pyruvate in VACV-infected cells deprived of glutamine. In addition, VACV-infected cells treated with increasing concentrations of BPTES exhibited a dose-dependent decrease in P4a levels compared to those of vehicle-treated (control) cells. The impact of BPTES treatment on viral protein synthesis was examined as early as 6 hpi and showed similar results (Fig. 3C). These data reveal that exogenous glutamine is necessary for VACV protein synthesis. Furthermore, these findings suggest that the need for glutamine extends beyond its role as an amino acid. When glutaminase is specifically inhibited, the utilization of glutamine as a TCA cycle intermediate is prevented, but glutamine is still available to be used as an amino acid. Therefore, the

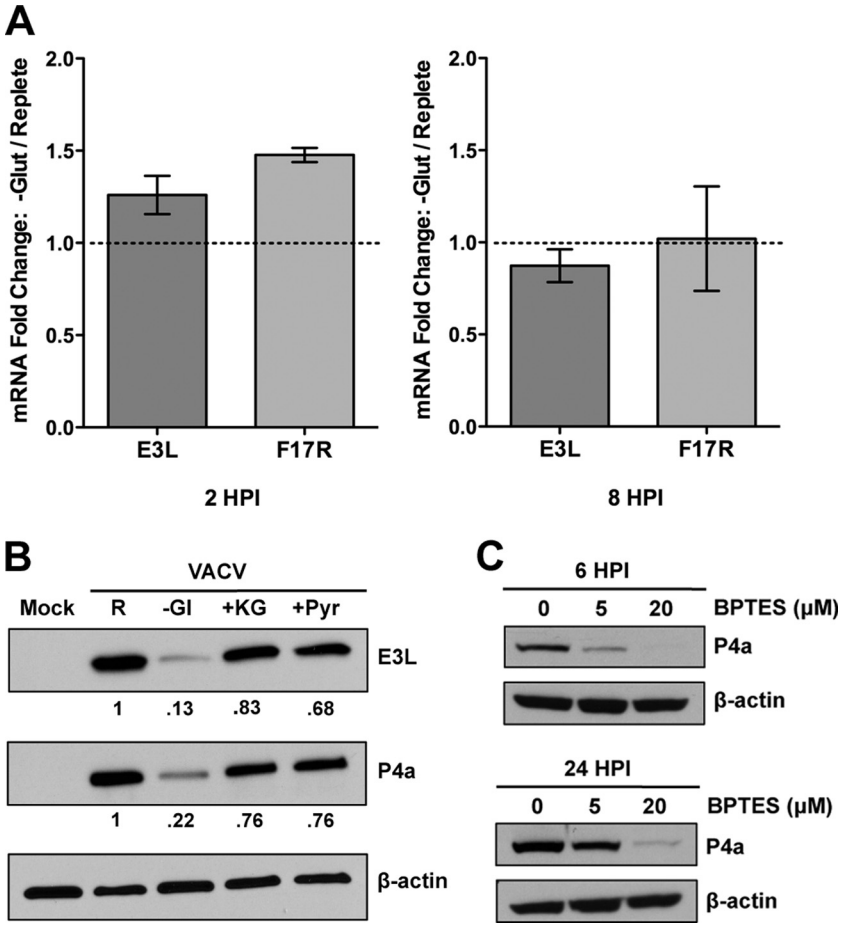

FIG 3 Glutamine is required to maintain the TCA cycle for VACV protein synthesis. (A) Quantitative real-time RT-PCR analysis of E3L and F17R transcript levels in VACV-infected cells supplemented with or without glutamine. HFFs were infected with VACV at an MOI of 5 and were fed replete medium or glutamine-free medium at 1 hpi. Viral mRNA expression was examined in cells harvested at 2 and 8 hpi. (B) Immunoblot analysis of E3L and P4a levels in VACV-infected cells fed replete medium (R), glutamine-free medium (−Gl), or glutamine-free medium supplemented with 7 mM dimethyl-α-ketoglutarate (KG) or 4 mM pyruvate (Pyr). Lysates from cells harvested at 24 hpi were subjected to Western blot analysis using antibodies against E3L, P4a, and the loading control β-actin. The values below the lanes indicate the relative intensity of each major band. (C) Immunoblot analysis of P4a levels in VACV-infected cells treated with increasing concentrations of BPTES. Cells were treated with 0, 5, or 20 μM BPTES at 1 hpi and harvested at 6 and 24 hpi for Western blot analysis.

requirement for glutamine during VACV infection is due largely to its use as an anaplerotic substrate to replenish the TCA cycle.

Levels of virion morphogenetic intermediates are reduced in glutamine-deprived infected cells. The above-described results show that glutamine is required at the stage of viral protein synthesis in the VACV life cycle. To determine if glutamine deprivation also affects VACV maturation, Western blot analysis was performed to measure P4a cleavage. P4a is a precursor polypeptide that is proteolytically cleaved to produce the major VACV core protein 4a and the protein p23 (28). The presence of these cleavage products serves as a marker for the conversion of immature virions (IVs) to MVs. As shown in Fig. 4A, although total protein levels were decreased in the absence of glutamine, the relative abundance of the cleavage product p23 was approximately equivalent to the relative abundance of the precursor P4a in glutamine-starved infected cells. These results suggest that glutamine deprivation does not inhibit VACV maturation.

To further investigate whether glutamine deprivation has an impact on VACV maturation, we next visualized virion morphogenesis by transmission electron microscopy (TEM). HFFs were infected with VACV at an MOI of 5 and fed replete medium, glutamine-free medium, or glutamine-free medium supplemented with 7 mM dimethyl-α-ketoglutarate. Cells were fixed at 24 hpi and prepared for examination by TEM. Figure 4B shows that no apparent block in VACV morphogenesis was observed in glutamine-deprived infected cells. All stages of virion morphogenesis were identified in VACV-infected cells under the three conditions, including crescents, IVs, and MVs. However, levels of these morphogenetic intermediates were strikingly reduced in VACV-infected cells starved of glutamine. Moreover, the addition of α-ketoglutarate to infected cells under glutamine-deprived conditions resulted in a significant recovery of levels of virion morphogenetic intermediates. Taken together, these data suggest that the drastic loss of VACV protein synthesis that occurs under glutamine-deprived conditions is responsible for the observed reduction in levels of virion morphogenetic intermediates and the overall decrease in infectious virus production.

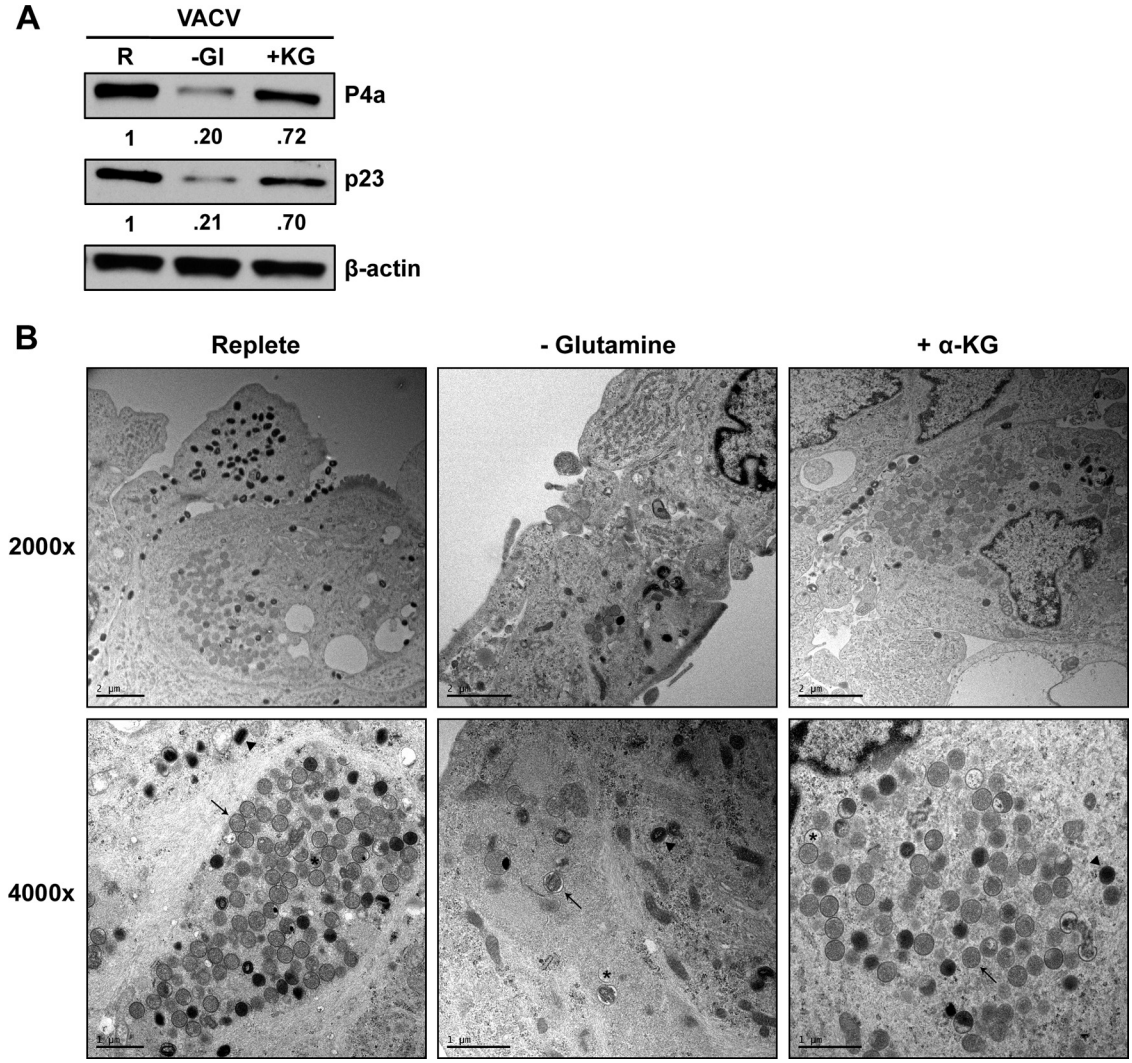

FIG 4 Glutamine deprivation results in reduced virion formation in VACV-infected cells. (A) Immunoblot analysis of P4a cleavage in VACV-infected cells fed replete medium, glutamine-free medium, or glutamine-free medium supplemented with 7 mM dimethyl-α-ketoglutarate. Lysates from cells harvested at 24 hpi were subjected to Western blot analysis using an antibody that recognizes both P4a and p23, a proteolytic product of P4a. The values below the lanes indicate the relative intensity of each major band. (B) Representative images of VACV morphogenesis in HFFs fed replete medium, glutamine-free medium, or glutamine-free medium supplemented with 7 mM dimethyl-α-ketoglutarate and processed for TEM at 24 hpi. Crescents (asterisks), immature virions (arrows), and mature virions (arrowheads) can be seen under all three conditions. The bottom left image was taken at a magnification of ×3,000 to include the entire virus factory.

DISCUSSION

Viruses have evolved to manipulate host cellular metabolism to support the energetic and biosynthetic requirements for successful replication. Utilizing a global metabolomic screen, we have found that several metabolic pathways are perturbed by VACV infection. Interestingly, we were surprised to find that VACV infection does not appear to induce glycolysis. As our laboratory and others have previously described, many different viruses activate glycolysis (1, 4–6, 29, 30), indicating an important role for this metabolic pathway during virus infection. In agreement with this, inhibition of glycolysis has been shown to attenuate both HCMV and HSV-1 replication as well as to induce apoptosis in cells latently infected with KSHV (29–32). Recently, it was reported that the VACV protein C16 stabilizes hypoxia-induced factor 1α (HIF-1α), resulting in the transcriptional upregulation of HIF-responsive genes, including two genes involved in glucose metabolism (33). However, the metabolic consequence of C16-induced HIF-1α stabilization in the context of VACV infection has yet to be investigated. In this study, we show that depriving VACV-infected cells of exogenous glucose has no significant impact on virus production, indicating that this carbon source is not essential for VACV replication.

Our metabolic screen identified a notable perturbation in glutamine metabolism during VACV infection. Glutamine levels are increased within the first 8 h of infection, while glutamate levels remain elevated throughout the course of infection. It is possible that the continued consumption of glutamine during VACV infection leads to the decrease in glutamine levels observed late in infection without lowering the intracellular pool of glutamate. For example, purine and pyrimidine biosynthetic pathways require the deamination of glutamine to glutamate to supply the nitrogen for these nucleotides. However, because glutamine is utilized as a

nitrogen source for both pathways, nucleotide biosynthesis results in the production and accumulation of glutamate (34). The steady elevated levels of glutamate observed in VACV-infected cells may indicate that glutamine is consumed in multiple metabolic pathways during infection, including those in which glutamate serves as a product and not as an intermediate. Consistent with this notion, levels of several biochemicals involved in purine and pyrimidine metabolism are significantly increased in VACV-infected cells (see Data Set S1 in the supplemental material). Further studies are in progress to assess global glutamine usage during VACV infection by metabolic carbon and nitrogen flux analysis.

In support of our metabolomic data, we show that the viral yield is drastically decreased when VACV-infected cells are deprived of exogenous glutamine, revealing that glutamine is the critical carbon source during VACV replication. Because glucose is not required to support glycolysis and the TCA cycle in VACV-infected cells, we hypothesized that glutamine is necessary for TCA cycle replenishment and ATP generation. Accordingly, we found that VACV production in glutamine-deprived cells is substantially rescued by supplementation with the TCA cycle intermediates α-ketoglutarate, oxaloacetic acid, and pyruvate. It is interesting to note that the ability of pyruvate to rescue virus production during glutamine deprivation suggests that VACV-infected cells can derive pyruvate from glutamine under normal conditions. The metabolic pathways involved in generating pyruvate from glutamine were not investigated here. However, similar results were observed when glutamine-starved HCMV-infected cells were fed pyruvate. It was speculated that this could occur when glutamine carbon enters the TCA cycle, via α-ketoglutarate, and proceeds to citrate. Citrate can then be shuttled to the cytoplasm and converted to oxaloacetic acid and acetyl coenzyme A (CoA), and oxaloacetic acid can ultimately be returned to pyruvate (8). Although TCA cycle intermediate supplementation significantly restored VACV production in glutamine-deprived cells, we did not observe a complete recovery of viral yield. As mentioned above, this may be due to the requirement for glutamine to support additional metabolic pathways during VACV infection, such as providing the nitrogen for nucleotide biosynthesis. Future work to determine the importance of other pathways of glutamine metabolism during VACV replication is warranted.

Our data also show that the anaplerotic usage of glutamine for the TCA cycle is crucial for viral protein synthesis. Translation is a highly energy-exhaustive process that requires ATP for both ribosome scanning of mRNA 5′ untranslated regions (UTRs) to initiate protein synthesis and the activation of amino acids during the elongation phase (35–37). Given that glutamine is a nonessential amino acid, and inhibition of glutaminolysis dramatically reduced VACV protein levels, our results suggest that glutamine may play a principal role during VACV infection by supplying the energy demand for viral protein synthesis. However, we cannot exclude the importance of glutamine utilization in the TCA cycle for providing the building blocks of protein synthesis, as several nonessential amino acids are biosynthesized from TCA cycle intermediates (reviewed in reference 38).

Why VACV induces such a striking alteration in carbon source utilization compared to other viruses investigated to date remains unknown. Glutamine is one of the most abundant amino acids in serum and, unlike glucose, which is solely a carbon source, additionally serves as a primary nitrogen donor for cells. Through its dual role in metabolism, glutamine may represent a more efficient nutrient to provide the ATP, macromolecular precursors, and reducing equivalents necessary for VACV replication (reviewed in references 10 and 39).

How glutaminolysis is induced by VACV is also currently not clear. We did not observe significant changes in the protein levels of the two glutaminolytic enzymes, glutaminase and glutamate dehydrogenase, during the course of VACV infection (K. A. Fontaine and M. Lagunoff, unpublished data). However, enzyme activity could be elevated without a corresponding increase in the protein expression level in VACV-infected cells. Current work is ongoing to elucidate the mechanism(s) through which VACV infection activates glutamine utilization. Given that glutamine metabolism is required for optimal VACV replication, inhibitors of glutaminolysis, such as BPTES or its newly designed analogs (40), may serve as novel therapies to target poxvirus infections. By broadening our understanding of how viruses alter host cellular metabolism, we hope to discover additional metabolic pathways that are critical to viral replication. This study is the first step in identifying the metabolic needs of poxviruses and could lead to future therapeutic avenues.

ACKNOWLEDGMENTS

We thank Stuart Isaacs (University of Pennsylvania) for providing anti-E3L and Dennis Hruby (Oregon State University) for providing anti-P4a. We also thank Adam Geballe (Fred Hutchinson Cancer Research Center) for reagents, Jacquelyn Braggin for technical assistance, and Almira Punjabi for helpful discussions.

M.L. was supported by grants from the NIAID, the NCI, and the NIDCR of the NIH under award numbers U54AI081680, RO1CA097934, and PO1DE021954. K.A.F. was supported in part by PHS NRSA T32 GM07270 from the NIGMS.

The content is solely the responsibility of the authors and does not necessarily represent the official views of the National Institutes of Health.

REFERENCES

1. **Munger J, Bajad SU, Coller HA, Shenk T, Rabinowitz JD.** 2006. Dynamics of the cellular metabolome during human cytomegalovirus infection. PLoS Pathog. **2:**e132. http://dx.doi.org/10.1371/journal.ppat.0020132.
2. **Munger J, Bennett BD, Parikh A, Feng XJ, McArdle J, Rabitz HA, Shenk T, Rabinowitz JD.** 2008. Systems-level metabolic flux profiling identifies fatty acid synthesis as a target for antiviral therapy. Nat. Biotechnol. **26:**1179–1186. http://dx.doi.org/10.1038/nbt.1500.
3. **Delgado T, Sanchez EL, Camarda R, Lagunoff M.** 2012. Global metabolic profiling of infection by an oncogenic virus: KSHV induces and requires lipogenesis for survival of latent infection. PLoS Pathog. **8:**e1002866. http://dx.doi.org/10.1371/journal.ppat.1002866.
4. **Vastag L, Koyuncu E, Grady SL, Shenk TE, Rabinowitz JD.** 2011. Divergent effects of human cytomegalovirus and herpes simplex virus-1 on cellular metabolism. PLoS Pathog. **7:**e1002124. http://dx.doi.org/10.1371/journal.ppat.1002124.
5. **Diamond DL, Syder AJ, Jacobs JM, Sorensen CM, Walters KA, Proll SC, McDermott JE, Gritsenko MA, Zhang Q, Zhao R, Metz TO, Camp DG, II, Waters KM, Smith RD, Rice CM, Katze MG.** 2010. Temporal proteome and lipidome profiles reveal hepatitis C virus-associated reprogramming of hepatocellular metabolism and bioenergetics. PLoS Pathog. **6:**e1000719. http://dx.doi.org/10.1371/journal.ppat.1000719.
6. **Hollenbaugh JA, Munger J, Kim B.** 2011. Metabolite profiles of human immunodeficiency virus infected CD4+ T cells and macrophages using LC-MS/MS analysis. Virology **415:**153–159. http://dx.doi.org/10.1016/j.virol.2011.04.007.
7. **Birungi G, Chen SM, Loy BP, Ng ML, Li SF.** 2010. Metabolomics approach for investigation of effects of dengue virus infection using the EA.hy926 cell line. J. Proteome Res. **9:**6523–6534. http://dx.doi.org/10.1021/pr100727m.
8. **Chambers JW, Maguire TG, Alwine JC.** 2010. Glutamine metabolism is essential for human cytomegalovirus infection. J. Virol. **84:**1867–1873. http://dx.doi.org/10.1128/JVI.02123-09.

9. **DeBerardinis RJ, Mancuso A, Daikhin E, Nissim I, Yudkoff M, Wehrli S, Thompson CB.** 2007. Beyond aerobic glycolysis: transformed cells can engage in glutamine metabolism that exceeds the requirement for protein and nucleotide synthesis. Proc. Natl. Acad. Sci. U. S. A. **104:**19345–19350. http://dx.doi.org/10.1073/pnas.0709747104.
10. **Deberardinis RJ, Sayed N, Ditsworth D, Thompson CB.** 2008. Brick by brick: metabolism and tumor cell growth. Curr. Opin. Genet. Dev. **18:**54–61. http://dx.doi.org/10.1016/j.gde.2008.02.003.
11. **Wise DR, DeBerardinis RJ, Mancuso A, Sayed N, Zhang XY, Pfeiffer HK, Nissim I, Daikhin E, Yudkoff M, McMahon SB, Thompson CB.** 2008. Myc regulates a transcriptional program that stimulates mitochondrial glutaminolysis and leads to glutamine addiction. Proc. Natl. Acad. Sci. U. S. A. **105:**18782–18787. http://dx.doi.org/10.1073/pnas.0810199105.
12. **Lewis VJ, Jr, Scott LV.** 1962. Nutritional requirements for the production of herpes simplex virus. I. Influence of glucose and glutamine of herpes simplex virus production by HeLa cells. J. Bacteriol. **83:**475–482.
13. **Eagle H, Habel K.** 1956. The nutritional requirements for the propagation of poliomyelitis virus by the HeLa cell. J. Exp. Med. **104:**271–287. http://dx.doi.org/10.1084/jem.104.2.271.
14. **Moss B.** 2001. Poxviridae: the viruses and their replication, p 2849–2883. *In* Knipe DM, Howley PM, Griffin DE, Lamb RA, Martin MA, Roizman B, Straus SE (ed), Fields virology, 4th ed. Lippincott Williams & Wilkins, Philadelphia, PA.
15. **Lewis-Jones S.** 2004. Zoonotic poxvirus infections in humans. Curr. Opin. Infect. Dis. **17:**81–89. http://dx.doi.org/10.1097/00001432-200404000-00003.
16. **Frey SE, Belshe RB.** 2004. Poxvirus zoonoses—putting pocks into context. N. Engl. J. Med. **350:**324–327. http://dx.doi.org/10.1056/NEJMp038208.
17. **Esposito JJ.** 2001. Poxviruses, p 2885–2921. *In* Knipe DM, Howley PM, Griffin DE, Lamb RA, Martin MA, Roizman B, Straus SE (ed), Fields virology, 4th ed. Lippincott Williams & Wilkins, Philadelphia, PA.
18. **Hutin YJ, Williams RJ, Malfait P, Pebody R, Loparev VN, Ropp SL, Rodriguez M, Knight JC, Tshioko FK, Khan AS, Szczeniowski MV, Esposito JJ.** 2001. Outbreak of human monkeypox, Democratic Republic of Congo, 1996 to 1997. Emerg. Infect. Dis. **7:**434–438. http://dx.doi.org/10.3201/eid0703.017311.
19. **Meyer H, Perrichot M, Stemmler M, Emmerich P, Schmitz H, Varaine F, Shungu R, Tshioko F, Formenty P.** 2002. Outbreaks of disease suspected of being due to human monkeypox virus infection in the Democratic Republic of Congo in 2001. J. Clin. Microbiol. **40:**2919–2921. http://dx.doi.org/10.1128/JCM.40.8.2919-2921.2002.
20. **Bradford MM.** 1976. A rapid and sensitive method for the quantitation of microgram quantities of protein utilizing the principle of protein-dye binding. Anal. Biochem. **72:**248–254.
21. **DiMaio TA, Gutierrez KD, Lagunoff M.** 2011. Latent KSHV infection of endothelial cells induces integrin beta3 to activate angiogenic phenotypes. PLoS Pathog. **7:**e1002424. http://dx.doi.org/10.1371/journal.ppat.1002424.
22. **Schneider CA, Rasband WS, Eliceiri KW.** 2012. NIH Image to ImageJ: 25 years of image analysis. Nat. Methods **9:**671–675. http://dx.doi.org/10.1038/nmeth.2089.
23. **Vander Heiden MG, Cantley LC, Thompson CB.** 2009. Understanding the Warburg effect: the metabolic requirements of cell proliferation. Science **324:**1029–1033. http://dx.doi.org/10.1126/science.1160809.
24. **Munoz-Pinedo C, El Mjiyad N, Ricci JE.** 2012. Cancer metabolism: current perspectives and future directions. Cell Death Dis. **3:**e248. http://dx.doi.org/10.1038/cddis.2011.123.
25. **Kim JW, Dang CV.** 2006. Cancer's molecular sweet tooth and the Warburg effect. Cancer Res. **66:**8927–8930. http://dx.doi.org/10.1158/0008-5472.CAN-06-1501.
26. **Pelicano H, Martin DS, Xu RH, Huang P.** 2006. Glycolysis inhibition for anticancer treatment. Oncogene **25:**4633–4646. http://dx.doi.org/10.1038/sj.onc.1209597.
27. **Yu Y, Clippinger AJ, Alwine JC.** 2011. Viral effects on metabolism: changes in glucose and glutamine utilization during human cytomegalovirus infection. Trends Microbiol. **19:**360–367. http://dx.doi.org/10.1016/j.tim.2011.04.002.
28. **Vanslyke JK, Whitehead SS, Wilson EM, Hruby DE.** 1991. The multistep proteolytic maturation pathway utilized by vaccinia virus P4a protein: a degenerate conserved cleavage motif within core proteins. Virology **183:**467–478. http://dx.doi.org/10.1016/0042-6822(91)90976-I.
29. **Delgado T, Carroll PA, Punjabi AS, Margineantu D, Hockenbery DM, Lagunoff M.** 2010. Induction of the Warburg effect by Kaposi's sarcoma herpesvirus is required for the maintenance of latently infected endothelial cells. Proc. Natl. Acad. Sci. U. S. A. **107:**10696–10701. http://dx.doi.org/10.1073/pnas.1004882107.
30. **McArdle J, Schafer XL, Munger J.** 2011. Inhibition of calmodulin-dependent kinase kinase blocks human cytomegalovirus-induced glycolytic activation and severely attenuates production of viral progeny. J. Virol. **85:**705–714. http://dx.doi.org/10.1128/JVI.01557-10.
31. **Radsak KD, Weder D.** 1981. Effect of 2-deoxy-D-glucose on cytomegalovirus-induced DNA synthesis in human fibroblasts. J. Gen. Virol. **57:**33–42. http://dx.doi.org/10.1099/0022-1317-57-1-33.
32. **Courtney RJ, Steiner SM, Benyesh-Melnick M.** 1973. Effects of 2-deoxy-D-glucose on herpes simplex virus replication. Virology **52:**447–455. http://dx.doi.org/10.1016/0042-6822(73)90340-1.
33. **Mazzon M, Peters NE, Loenarz C, Krysztofinska EM, Ember SW, Ferguson BJ, Smith GL.** 2013. A mechanism for induction of a hypoxic response by vaccinia virus. Proc. Natl. Acad. Sci. U. S. A. **110:**12444–12449. http://dx.doi.org/10.1073/pnas.1302140110.
34. **Cory J.** 2006. Purine and pyrimidine nucleotide metabolism, p 789–822. *In* Devlin T (ed), Textbook of biochemistry with clinical correlations, 6th ed. Wiley-Liss, Hoboken, NJ.
35. **Pestova TV, Kolupaeva VG.** 2002. The roles of individual eukaryotic translation initiation factors in ribosomal scanning and initiation codon selection. Genes Dev. **16:**2906–2922. http://dx.doi.org/10.1101/gad.1020902.
36. **Jackson RJ.** 1991. The ATP requirement for initiation of eukaryotic translation varies according to the mRNA species. Eur. J. Biochem. **200:**285–294. http://dx.doi.org/10.1111/j.1432-1033.1991.tb16184.x.
37. **Alberts B, Johnson A, Lewis J, Raff M, Roberts K, Walter P.** 2002. Molecular biology of the cell, 4th ed. Garland Science, New York, NY.
38. **Berg JM, Tymoczko JL, Stryer L.** 2002. Biochemistry, 5th ed. WH Freeman, New York, NY.
39. **Lu W, Pelicano H, Huang P.** 2010. Cancer metabolism: is glutamine sweeter than glucose? Cancer Cell **18:**199–200. http://dx.doi.org/10.1016/j.ccr.2010.08.017.
40. **Shukla K, Ferraris DV, Thomas AG, Stathis M, Duvall B, Delahanty G, Alt J, Rais R, Rojas C, Gao P, Xiang Y, Dang CV, Slusher BS, Tsukamoto T.** 2012. Design, synthesis, and pharmacological evaluation of bis-2-(5-phenylacetamido-1,2,4-thiadiazol-2-yl)ethyl sulfide 3 (BPTES) analogs as glutaminase inhibitors. J. Med. Chem. **55:**10551–10563. http://dx.doi.org/10.1021/jm301191p.